Progress In Electromagnetics Research C, Vol. 113, 123–136, 2021

Design of Compact 4-Port MIMO Antenna Based on Minkowski Fractal Shape DGS for 5G Applications

Sara Yehia Abdel Fatah[1, *], Ehab K. I. Hamad[2], Wael Swelam[3], A. M. M. A. Allam[4], and Hesham A. Mohamed[5]

Abstract—A 4-port wideband Multiple-Input Multiple-Output (MIMO) antenna operating in the frequency band from 24.8 GHz to 27.6 GHz dedicated to 5G application is proposed in this manuscript. The MIMO antenna is implemented on a $23.75 \times 42.5 \times 0.508\,\text{mm}^3$ Roger/Druoid 5880 substrate with relative dielectric constant $\epsilon_r = 2.2$ and loss tangent 0.0009. Firstly, the design starts with a simulation and optimization of a single element antenna based on Minkowski fractal shape as Defected Ground Structures (DGSs) using CST Studio Suite. The single proposed element shows a 7 dBi gain and antenna efficiency of 85% at the operating frequency band. Secondly, to design a MIMO antenna with good isolation, three different configurations are used, and overall MIMO performances such as low Envelope Correlation Coefficient (ECC), high Diversity gain (DG), and low Channel Capacity Loss (CCL) are calculated and analyzed. Finally, fabrication and measurement are conducted to validate the concept for single and 2-port MIMO antenna performance.

1. INTRODUCTION

5G communication systems development requires a high data transmission rate and stable signal quality [1]. However, the millimeter-wave (mm-wave) spectrum dedicated to 5G application shows some challenge limitations such as signal fading, atmospheric absorptions, and path loss attenuations which are more significant using a single antenna element [2–4]. One of the researchers' proposed technology solutions is the use of Multiple-Input-Multiple-Output (MIMO), as it enables channel capacity, high data rates, and throughput improvement [5–7]. During the development of the 5th generation MIMO antenna, three main requirements related to mm-wave spectrum are needed, which must be taken into consideration, high bandwidth, high gain related to atmospheric diminutions and absorptions, and finally, a low-profile overall structure so that it can be easily integrated into a MIMO system.

Another constraint that has a very strong impact on the coupling between MIMO antenna elements and should be considered is the distance between elements. This distance should be chosen at a minimum between $\lambda/4$ and $\lambda/2$ to have a mutual coupling less than -15 dB and therefore have an efficient working MIMO system. From another part, greater distance between antenna elements leads to greater overall MIMO antenna size. Consequently, a compromise between the overall MIMO systems and mutual coupling minimization should be considered during the MIMO antenna design process. Reduction in mutual coupling means low Envelope Correlation Coefficient (ECC), high Diversity gain (DG), and low Channel Capacity Loss (CCL).

Received 27 April 2021, Accepted 5 June 2021, Scheduled 16 June 2021
* Corresponding author: Sara Yehia Abdel Fatah (Phd-ecu-S@hotmail.com).
[1] Department of Mechatronics Engineering and Automation, Faculty of Engineering, Egyptian Chinese University, Cairo, Egypt. [2] Department of Electrical Engineering, Faculty of Engineering, Aswan University, Aswan, Egypt. [3] Department of Electronics and Communications Engineering, Arab Academy for Science, Technology and Maritime Transport, Cairo, Egypt. [4] Department of Communication Engineering, German University in Cairo, Cairo, Egypt. [5] Department of Microstrip, Electronics Research Institute (ERI), Giza, Egypt.

Various techniques and procedures are presented in the literature with multiple MIMO antenna designs to minimize the mutual coupling between MIMO antenna element keeping the MIMO overall size small such as the use of Multi-Mode Resonator (MMR) in [8] where the isolation was below 15 dB, and the overall size was $6 \times 6\,\text{cm}^2$. In [9], a neutralization line is used for isolation improvement between MIMO antenna elements. A decoupling circuit network and structure is used in [10, 11] to connect antenna elements and reduce the coupling and improve MIMO antenna performance. Another procedure based on two long stubs and short strip defected ground structures, with a good insertion loss below -15 dB between MIMO antenna elements and the size of $2.6 \times 4\,\text{cm}^2$ is reported in [12]. A U-shaped MIMO antenna for a 5G mobile application with a good isolation of 19 dB is achieved using two vertical open stubs [13]. A dual-band MIMO self-decoupled antenna showing isolation better than 17.5 dB based on grounded elements is introduced in [14].

Orthogonal polarization is a very well-known technique used by researchers to merge many antennas in a limited space with good isolation and performance; as presented in [15, 16], good performances are obtained. Microstrip patch antennas have a drawback of narrow bandwidth. To enhance the operating bandwidth and multiband design antenna, researchers tend to use different techniques such as DGS, Metamaterial, slot, and fractal-based methods [17–26].

A combined technique based on both DGS and fractal methods is used to create a multiband antenna with broadband bandwidth. Mandelbrot firstly introduced fractal geometries in 1975 as inspiration from clouds, mountains, plant leaves, and coastlines [27–29]. Multiple fractal-based antenna geometries exist in literature based on the following main basic geometries: Koch Snowflake, Sierpinski gasket, Sierpinski carpet, Hilbert, and Minkowski Island are the basic fractal antenna geometries [30, 31].

A 4-port wideband MIMO antenna based on Minkowski fractals shape DGS is presented in this manuscript. The design process starts with a classical patch antenna design, then a Minkowski fractals shape DGS (MF-DGS) is slotted on the ground layer as a second step. Lastly, the Minkowski fractals shape DGS based antenna is taken as a reference element for different MIMO antenna configuration designs. Reference antenna design procedure is discussed in Section 2. MIMO antenna design procedure and performance analysis discussion are in Sections 3, 4, and 5. Finally, the conclusion is given in Section 6.

2. ANTENNA DESIGN PROCEDURE

The overall proposed MIMO antenna is mounted on a $23.75 \times 42.5 \times 0.508\,\text{mm}^3$ Roger/Druoid 5880 substrate with a relative dielectric constant of $\epsilon_r = 2.2$. Reference single antenna element has an overall dimension of $23.75 \times 18.75 \times 0.508\,\text{mm}^3$. The reference single and MIMO antenna design procedures are explained in Subsections 2.1 and 2.2.

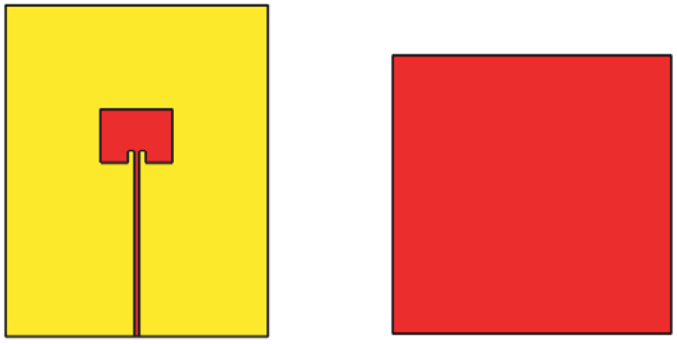

Figure 1. Basic patch antenna without Minkowski fractal shape.

2.1. Proposed Reference Single Antenna Element

The reference single antenna element design procedure is divided into three main steps. Firstly, as shown in Figure 1, a simple rectangular patch antenna with full ground connected to a 50-ohm microstrip line feed using reference Equations (1)–(4) is designed.

$$W = \frac{c_o}{2f_r}\sqrt{\frac{2}{\epsilon_r + 1}} \tag{1}$$

$$L = \frac{c_o}{2f_r\sqrt{\epsilon_{reff}}} - 2\Delta L \tag{2}$$

$$\Delta L = 0.412h\frac{(\epsilon_{reff} + 0.3)}{(\epsilon_{reff} - 0.258)}\frac{\left(\frac{W}{h} + 0.264\right)}{\left(\frac{W}{h} + 0.8\right)} \tag{3}$$

$$\epsilon_{reff} = \frac{(\epsilon_r + 1)}{2} + \frac{(\epsilon_r - 1)}{2}\left[1 + 12\frac{h}{W}\right]^{-1/2} \tag{4}$$

As the second step, a second iteration Minkowski fractal shape is slotted in the ground plane based on the DGS technique to introduce multiple resonances due to the effect of the distribution in the ground surface current, which leads to an enhancement of the bandwidth frequency. The proposed Minkowski fractal shapes evolution process is illustrated in Figure 2. The optimal results antenna structure with MF-DGS is considered the reference antenna element of the overall MIMO antenna. Overall dimension values are illustrated in Table 1, and both simulation and fabricated antenna structure are sketched in Figure 3.

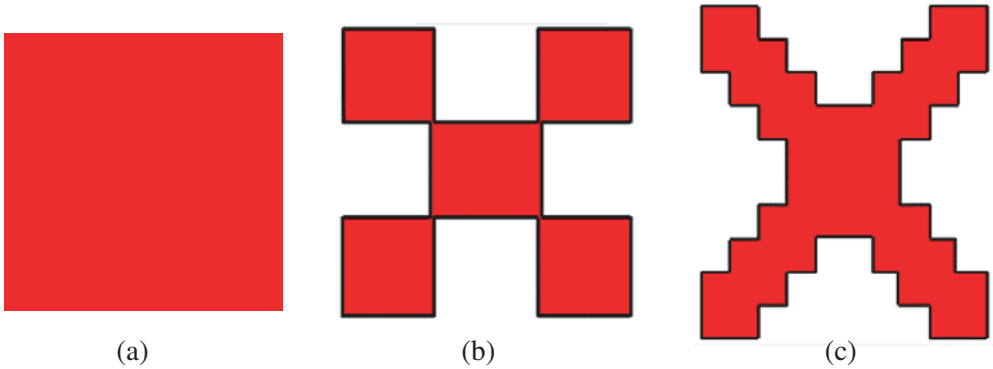

Figure 2. Minkowski fractal shapes evolution process. (a) Basic. (b) First iteration. (c) Second iteration.

Table 1. Design parameters of the proposed dual-band antenna.

Variables	$L1$	$W1$	$L2$	$W2$	Lf
Values (mm)	23.75	18.75	3.80	5.15	12.47
Variables	G	$Fr01$	$Fr02$	$Fr03$	$Fr04$
Values (mm)	0.83	0.88	1.95	5	2.5

Adding MF-DGS to the basic patch antenna led to the creation of multiple resonance frequencies adjacent to each other generated related to multiple Minkowski fractal edges that lead to the enhancement of the bandwidth operating frequency of the basic reference element from 23–24 GHz to 24.8–27.6 GHz with a good return loss of 30 dB as illustrated in Figure 4. As shown in Figure 5 and

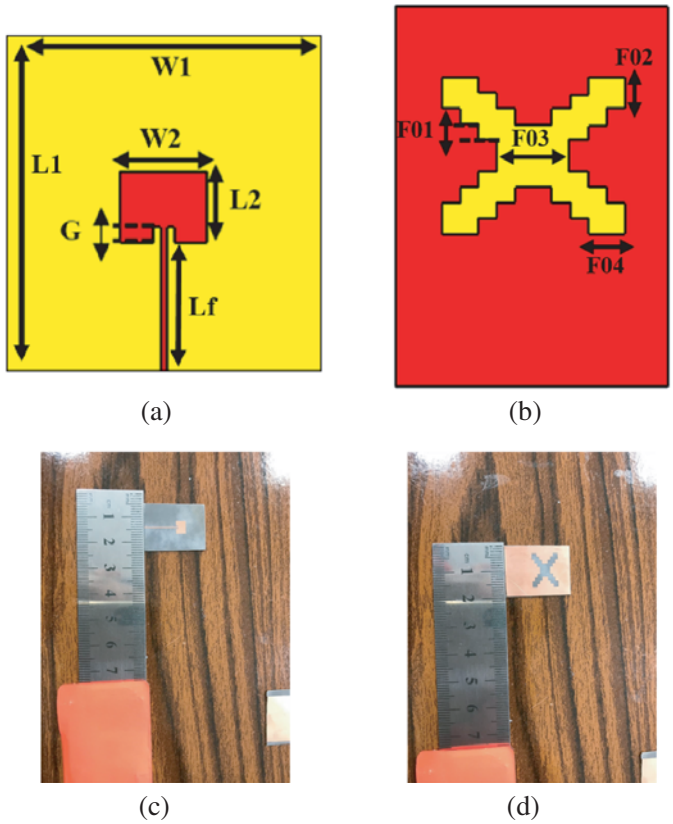

Figure 3. Basic patch antenna with MF-DGS. (a) Simulated top view. (b) Simulated bottom view. (c) Fabricated top view. (d) Fabricated bottom view.

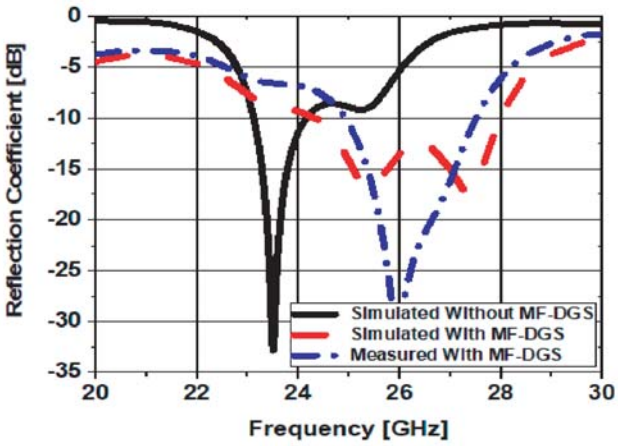

Figure 4. Simulated and measured reflection coefficient for patch with & without MF-DGS.

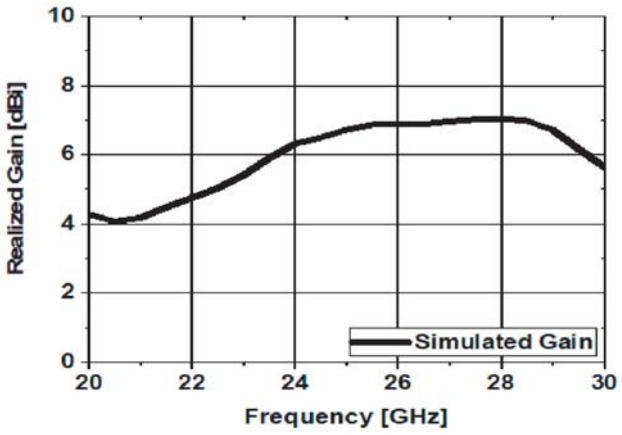

Figure 5. Simulated realized gain with MF-DGS.

Figure 6, the proposed MF-DGS based single antenna achieves a gain of 7 dBi and antenna efficiency of 85% at the operating frequency bands, which is suitable for the 5G application. Lastly, radiation pattern with $\phi = 0°$ and $\phi = 90°$ is sketched in Figure 7, and nearly omnidirectional behaviour is noticed.

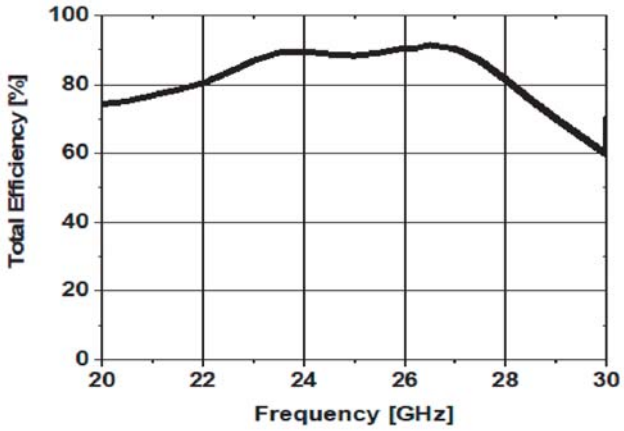

Figure 6. Simulated antenna efficiency with MF-DGS.

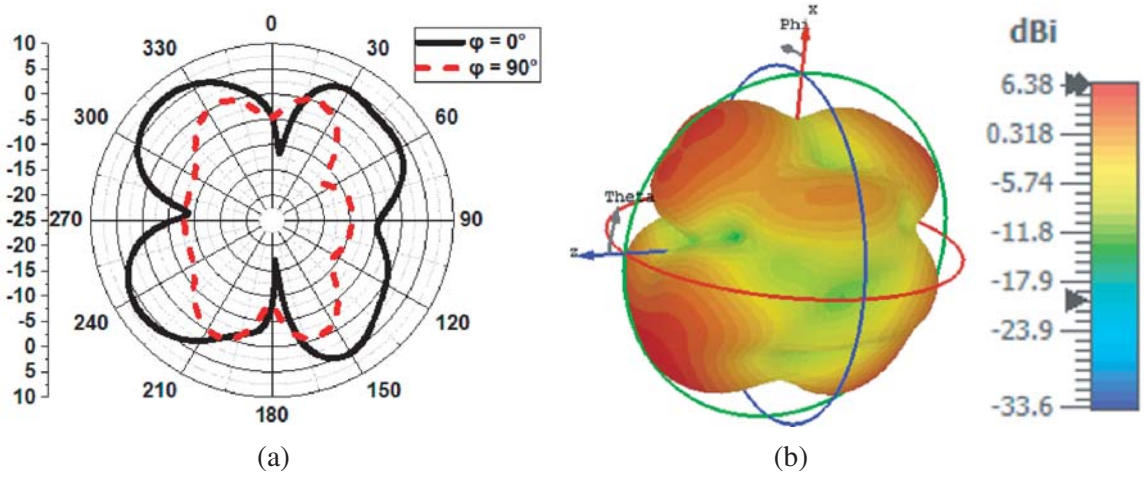

Figure 7. Simulated radiation patterns with MF-DGS. (a) 2D polar radiation patterns $\phi = 0°$ and $\phi = 90°$. (b) 3D radiation patterns.

2.2. Proposed MIMO Antenna

To design a 4-port MIMO antenna, we start with the design of three different 2-port MIMO configurations, including polarization diversity as represented in Figure 8. Basic single elements in the MIMO configuration are spaced approximately $\lambda/2$ (11 mm at 26 GHz) apart to ensure good performance and isolation achievement.

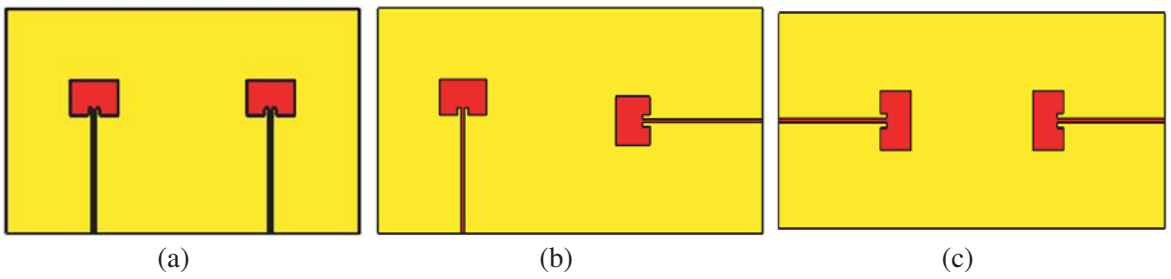

Figure 8. Three proposed MIMO antenna configurations. (a) Configuration 01. (b) Configuration 02. (c) Configuration 03.

The proposed three different configurations operate from 24.8 GHz to 27.6 GHz frequencies as exhibited in Figure 9. As observed from Figure 9, the reduction of mutual coupling between antenna elements is optimal in configuration 01 with good isolation of approximately 25 dB at the operating band frequency compared to the mutual coupling in configuration 02 achieving the isolation of approximately 20 dB. In contrast, configuration 03 shows a higher isolation than the two previous configurations.

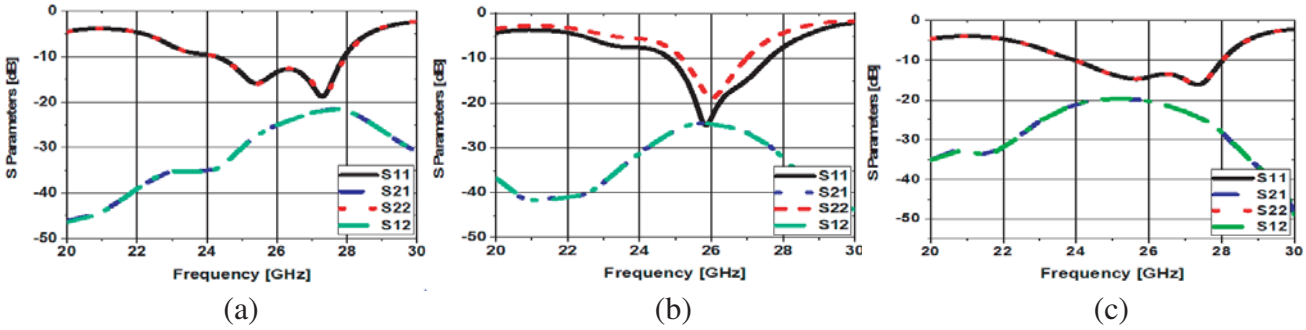

Figure 9. Scattering parameter for MIMO antenna configurations. (a) Configuration 01. (b) Configuration 02. (c) Configuration 03.

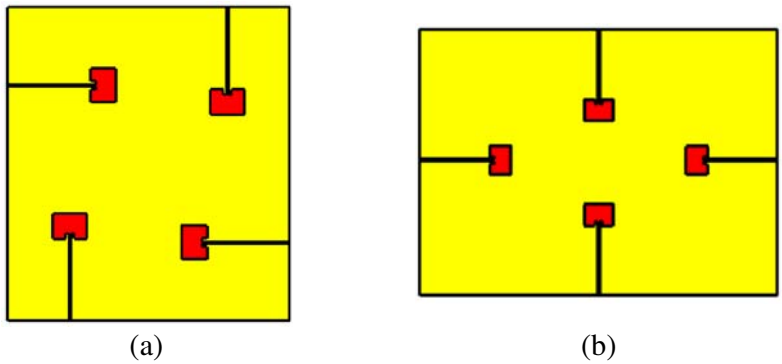

Figure 10. 4-port MIMO antenna configurations. (a) Configuration 02 based MIMO. (b) Configuration 03.

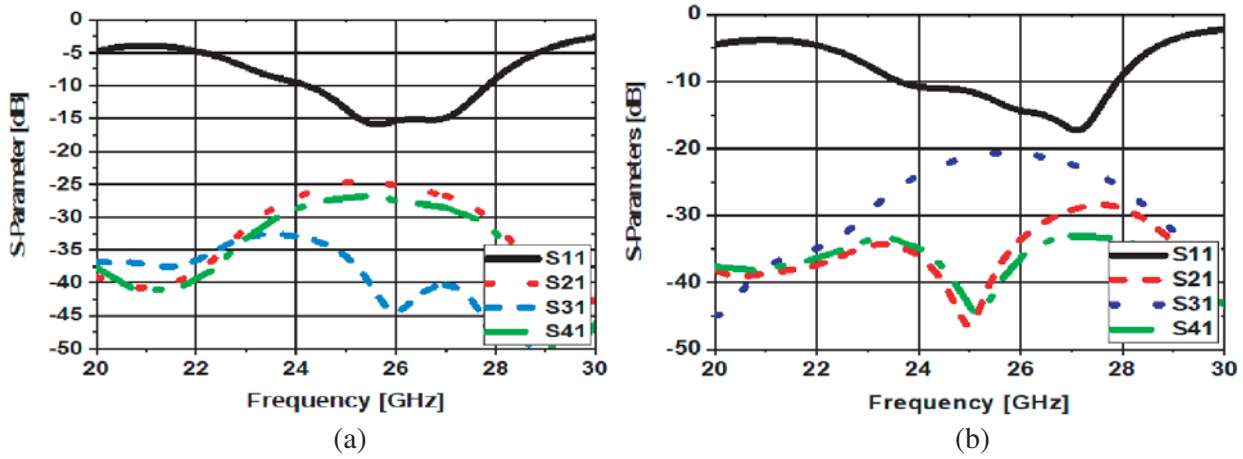

Figure 11. Scattering parameter for 4-port MIMO antenna. (a) Configuration 02 based MIMO. (b) Configuration 03.

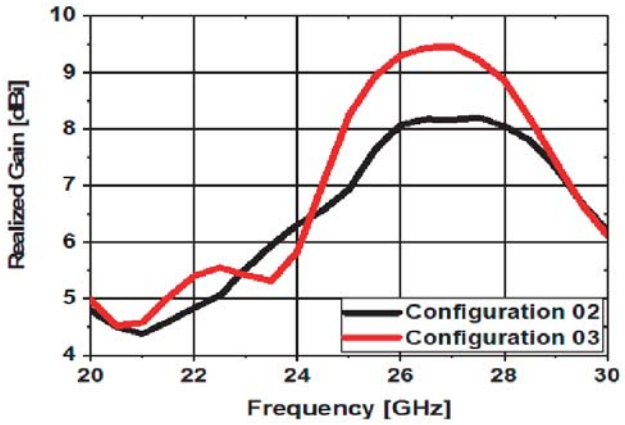

Figure 12. Simulated realized gain 4-port MIMO antenna.

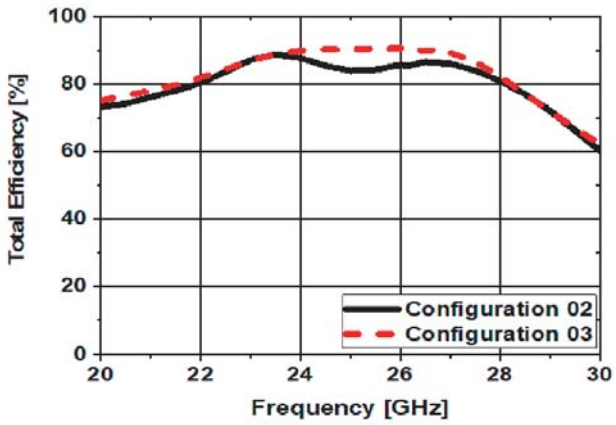

Figure 13. Simulated total efficiency for 4-port MIMO antenna.

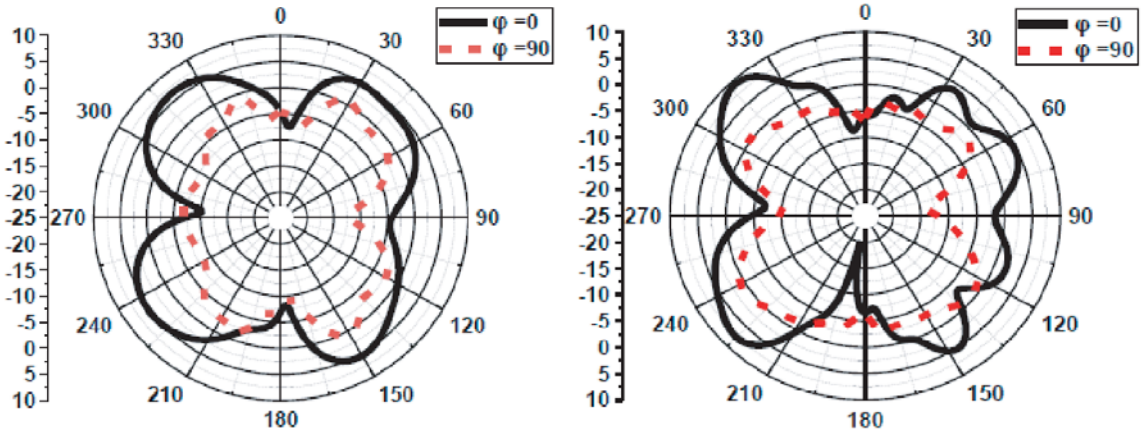

Figure 14. Simulated radiation patterns for 4-port MIMO antenna $\phi = 0°$ and $\phi = 90°$. (a) Configuration 02. (b) Configuration 03.

However, due to the used connectors' measurement limitations, configuration 02 and configuration 03 are selected for designing a 4-port MIMO antenna, as shown in Figure 10, and the reflection coefficient is reported in Figure 11. The 4-port MIMO antenna shows a gain of 8.25 dB and 9.5 dB for both configuration 02 and configuration 03, as illustrated in Figure 12. The total efficiencies of 85% and 90% for the two different configurations 02 and 03 are shown in Figure 13. Lastly, a nearly omnidirectional radiation pattern is noticed for both configuration 02 and configuration 03, as shown in Figure 14, which is suitable for our target application as a 5G base station hotspot.

3. PROPOSED MIMO ANTENNA PERFORMANCE ANALYSIS

In addition to the basic antenna parameters (S-parameters, gain, and antenna efficiency), additional MIMO performance parameters such as ECC, DG, and CCL for the MIMO antenna configuration are calculated and analyzed as illustrated in Figure 18, Figure 19, and Figure 20, respectively.

3.1. Channel Capacity Loss (CCL)

In literature it is noticed that the optimum value of CCL is CCL < 0.4 b/s/Hz [32]. It is calculated using the following equation:

$$CCL = \log_2\left(\det\left(\psi^R\right)\right) \tag{5}$$

where

$$\begin{aligned}\left(\psi^R\right) &= \begin{bmatrix} \rho_{11} & \rho_{12} \\ \rho_{21} & \rho_{22} \end{bmatrix} \\ \rho_{ii} &= 1 - \left(|S_{ii}|^2 + |S_{ij}|^2\right) \\ \rho_{ii} &= -\left(S_{ii}^* S_{ij} + S_{ji}^* S_{ij}\right) \text{ for i and j = 1 and 2}\end{aligned}$$

The CCL is depicted in Figure 15 for 2-port configuration and 4-port MIMO antenna. Concerning the 2-port MIMO system, it is clear that the measured CCL is larger than the simulated one in most of the frequency band except from 22 to 24 GHz. On the other hand, the 4-port one noticed that the CCL is lower than the 2-port.

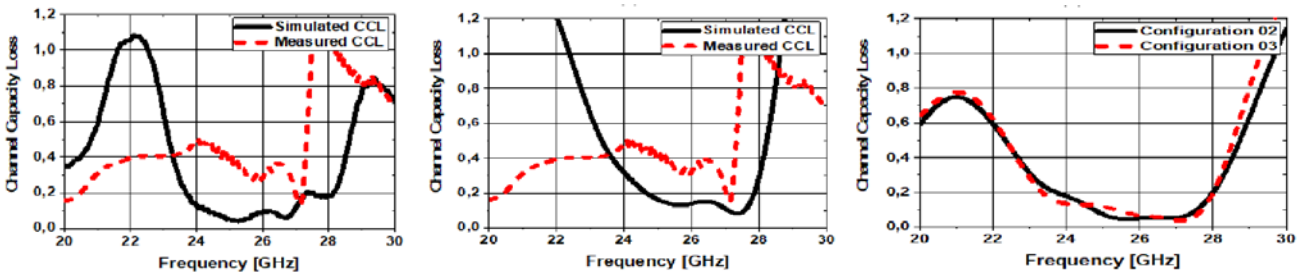

Figure 15. Channel capacity loss (CCL) for 2-port and 4-port MIMO antenna. (a) Configuration 02 (2-port). (b) Configuration 03 (2-port). (c) Simulated 4-port MIMO.

3.2. Envelope Correlation Coefficient (ECC)

Equation (6) [33] presents the ECC MIMO antenna essential parameter used to analyze the overall antenna performance. Figure 16 illustrates the simulated and measured ECCs for configuration 02 and configuration 03 for both 2-port and 4-port MIMO antennas. It can be noticed that the ECC values are below 0.005 for both configurations in both MIMO cases (Below the nominal standard value of 0.5) throughout the band; hence configuration 02 shows a better correlation than configuration 03.

$$ECC = \frac{\left|\int \left(XPR \cdot E_{\theta 1}\left(\Omega\right) E_{\theta 2}^*\left(\Omega\right) + E_{\phi 1}\left(\Omega\right) E_{\phi 2}^*\left(\Omega\right) d\Omega\right)\right|^2}{\int \left(XPR \cdot G_{\theta 1}\left(\Omega\right) E_{\phi 1}^*\left(\Omega\right)\right) d\Omega \cdot \int \left(XPR \cdot G_{\theta 2}\left(\Omega\right) E_{\phi 2}^*\left(\Omega\right)\right) d\Omega} \tag{6}$$

3.3. Diversity Gain (DG)

Equation (7) [34] illustrates another MIMO antenna essential parameter described as transmission power losses in terms of diversity gain. The simulated and measured DG values for 2-port and 4-port MIMO antennas (configuration 02 and configuration 03) are approximately 9.9 dB over the band, as reported in Figure 17. It is clear that the results confirm a satisfactory diversity performance of the proposed MIMO antenna structures with different configurations.

$$DG = 10\sqrt{1 - ECC} \tag{7}$$

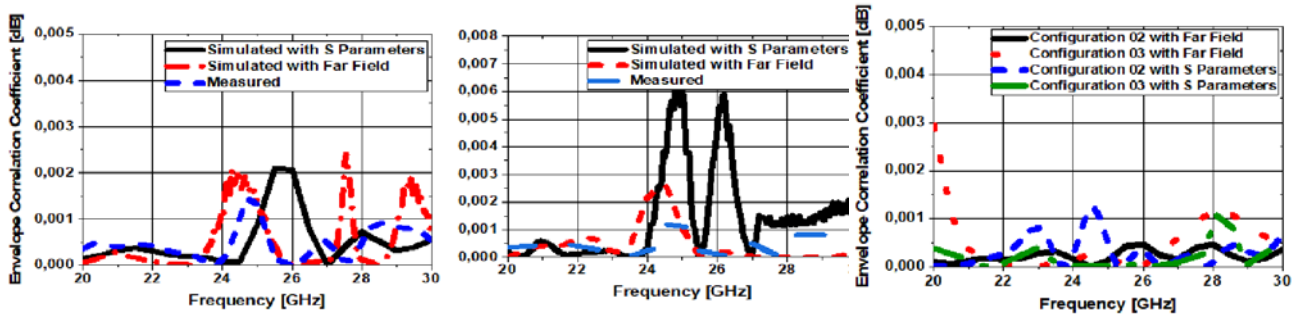

(a) (b) (c)

Figure 16. Envelope correlation coefficient (ECC) for 2-port and 4-port MIMO antenna. (a) Configuration 02 (2-port). (b) Configuration 03 (2-port). (c) Simulated 4-port MIMO.

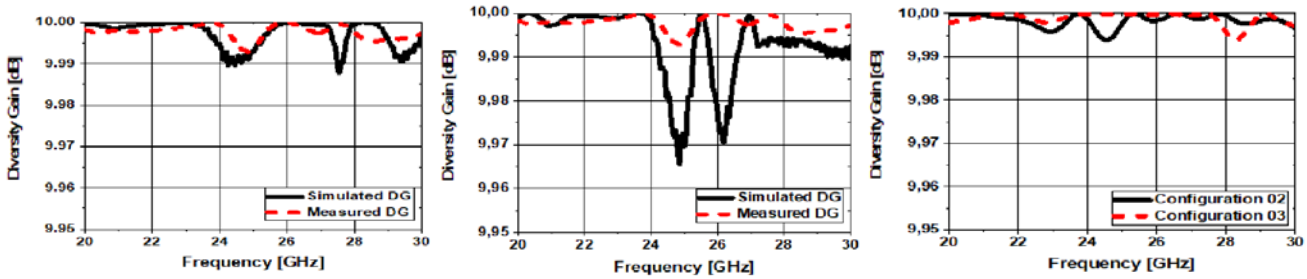

(a) (b) (c)

Figure 17. Diversity gain (DG) for 2-port and 4-port MIMO antenna. (a) Configuration 02 (2-port). (b) Configuration 03 (2-port). (c) Simulated 4-port MIMO.

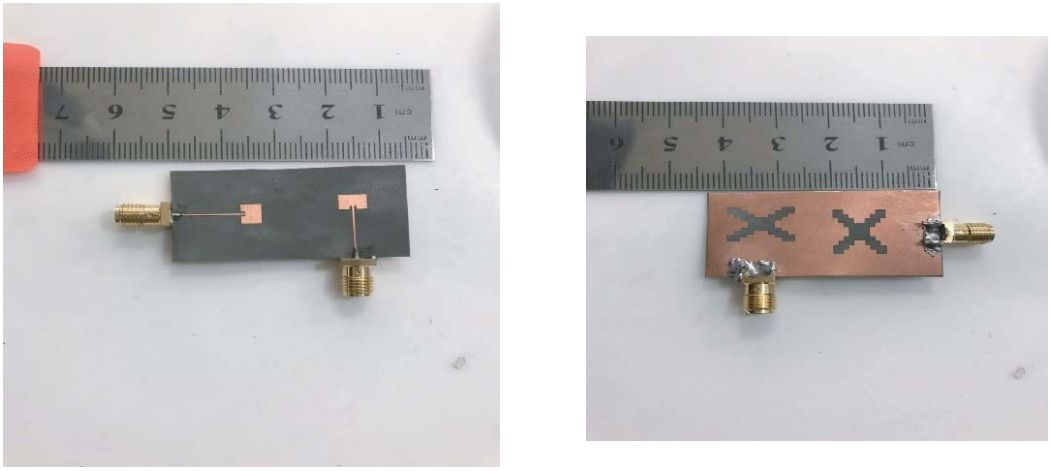

(a) (b)

Figure 18. Fabricated 2-port MIMO antenna structures 02. (a) Top view. (b) Bottom view.

4. FABRICATED AND MEASUREMENT RESULTS

Figure 18 and Figure 19 present the fabricated 2-port MIMO antenna configuration 02 and configuration 03, and Figure 20 illustrates the measured S-parameters of that last fabricated 2-port MIMO antenna. As can be noticed, an acceptable agreement with simulated results is achieved.

5. COMPARISON WITH OTHER RELATED WORKS

Comparative analysis of the proposed MIMO antenna with other related works is conducted and described in Table 2. It is observed that the proposed MIMO antenna exhibits better overall performance in terms of bandwidth, gain, ECC, and DG. Furthermore, it presents a low profile and overall compactness structure compared to other published works. Hence, the proposed MIMO antenna configuration is more than suitable for 5G mm-wave applications.

Table 2. Proposed antenna's performance comparison with other related works.

References	Frequency (GHz) & Application	Overall Dimension (λ^2)	Gain (dBi)	DG, ECC & CCL (dB)
[34]	25	2.75×1.73	7.37	NA
[35]	28	2.5×2.9	8.3	0.01 9.96 NA
[36]	28	1.65×1.65	8	0.13 9.9 NA
[37]	27.5	2.72×3.18	8.3	< 0.01 > 9.96 NA
[38]	24	1.2×1.52	6	0.24 9.7 NA
[39]	28	1.72×1.72	14	NA
[40]	26	2.6×2.6	7.4	NA
[41]	34	19.75×9.72	5.8–7.2	< 0.001 NA
[42]	28	6.8×10	5.13	0.05
[43]	28	5×10	NA	< 0.002 NA NA
Simulated 4-Port (Config 02)	26	4.13×4.13	8	< 0.002 9.9 < 0.001
Simulated 4-Port (Config 03)	26	4.13×5.54	9	< 0.002 9.9 < 0.001
Fabricated 2-Port (Config 02)	26	2.065×2.065	8.25	< 0.001 9.9 < 0.001
Fabricated 2-Port (Config 03)	26	2.065×2.77	9.5	< 0.001 9.9 < 0.001

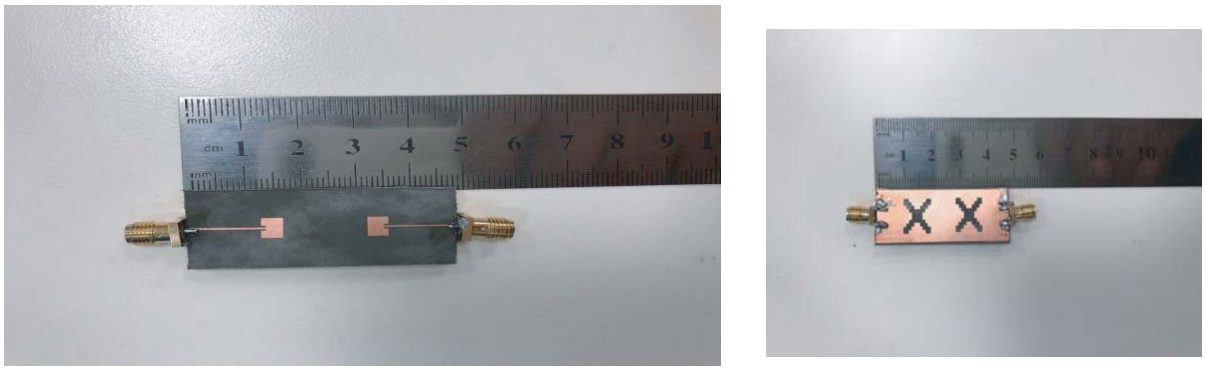

(a) (b)

Figure 19. Fabricated proposed 2-port MIMO antenna structures 03. (a) Top view. (b) Bottom view.

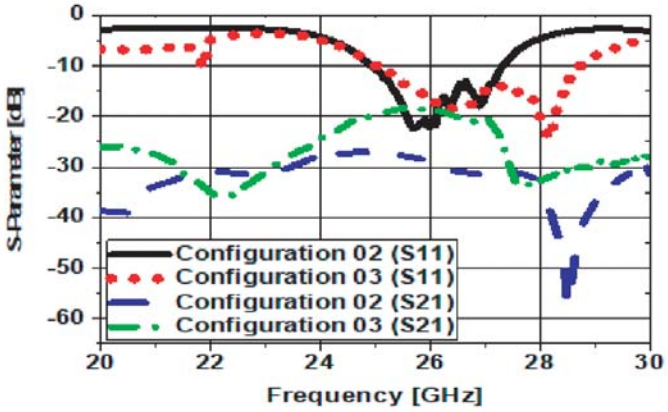

Figure 20. Measured S-parameter of the 2-port MIMO antenna.

6. CONCLUSION

In this work, a wideband MIMO antenna based on MF-DGS is proposed for 5G mm-wave applications. Firstly, a basic patch antenna with slotted MF-DGS is designed and analyzed. The effect of MF-DGS on the basic patch antenna without MF-DGS leads to the creation of multiple resonance frequencies adjacent to each other generated by Minkowski fractal edges that lead to the enhancement of the bandwidth operating frequency band of the basic reference element from 23–24 GHz to 24.8–27.6 GHz.

Secondly, three different 2-port MIMO configurations, namely configuration 01, configuration 02, and configuration 03, are designed and analyzed. However, due to measurement limitations, configuration 02 and configuration 03 are selected to design the 4-port MIMO antenna structure. The proposed design of the 2-port MIMO antenna operates at frequency bands from 24.8 to 27.6 GHz in both chosen configurations. Moreover, the obtained realized gain of the proposed two configurations is 8.25 dBi, 9.5 dBi, and antenna efficiency is 87% for both configurations at the operating frequency band. It is noticed that the DG shows a high value of 9.9, and the calculated ECC and CCL < 0.001, which is suitable for MIMO application in 5G mm-wave band.

REFERENCES

1. Mak, K. M., H. W. Lai, K. M. Luk, and C. H. Chan, "Circularly polarized patch antenna for future 5G mobile phones," *IEEE Access*, Vol. 2, 1521–1529, 2014.

2. Kumar, S., A. S. Dixit, R. R. Malekar, H. D. Raut, and L. K. Shevada, "Fifth generation antennas: A comprehensive review of design and performance enhancement techniques," *IEEE Access*, Vol. 8, 163 568–163 593, 2020.
3. Shayea, I., T. A. Rahman, M. H. Azmi, and M. R. Islam, "Real measurement study for rain rate and rain attenuation conducted over 26 GHz microwave 5G link system in malaysia," *IEEE Access*, Vol. 6, 19 044–19 064, 2018.
4. Fatah, S. Y. A., E. K. Hamad, W. Swelam, A. Allam, M. F. A. Sree, and H. A. Mohamed, "Design and implementation of UWB slot-loaded printed antenna for microwave and millimeter wave applications," *IEEE Access*, Vol. 9, 29 555–29 564, 2021.
5. Rahman, M., M. NagshvarianJahromi, S. S. Mirjavadi, and A. M. Hamouda, "Compact UWB band-notched antenna with integrated bluetooth for personal wireless communication and UWB applications," *Electronics*, Vol. 8, No. 2, 158, 2019.
6. Marzouk, H. M., M. I. Ahmed, and A. H. A. Shaalan, "Novel dual-band 28/38 GHz MIMO antennas for 5G mobile applications," *Progress In Electromagnetics Research C*, Vol. 93, 103–117, 2019.
7. Ghouz, H. H. M., M. F. A. Sree, and M. A. Ibrahim, "Novel wideband microstrip monopole antenna designs for WiFi/LTE/WiMax devices," *IEEE Access*, Vol. 8, 9532–9539, 2020.
8. Ojaroudi Parchin, N., H. Jahanbakhsh Basherlou, M. Alibakhshikenari, Y. Ojaroudi Parchin, Y. I. Al-Yasir, R. A. Abd-Alhameed, and E. Limiti, "Mobile-phone antenna array with diamond-ring slot elements for 5G massive MIMO systems," *Electronics*, Vol. 8, No. 5, 521, 2019.
9. Kiem, N. K., H. N. B. Phuong, and D. N. Chien, "Design of compact 4×4 UWB-MIMO antenna with WLAN band rejection," *International Journal of Antennas and Propagation*, Vol. 2014, 2014.
10. Abdalla, M. A. and A. A. Ibrahim, "Compact and closely spaced metamaterial MIMO antenna with high isolation for wireless applications," *IEEE Antennas and Wireless Propagation Letters*, Vol. 12, 1452–1455, 2013.
11. Zou, X.-J., G.-M. Wang, Y.-W. Wang, and B.-F. Zong, "Mutual coupling reduction of quasi-Yagi antenna array with hybrid wideband decoupling structure," *AEU — International Journal of Electronics and Communications*, Vol. 129, 153553, 2021.
12. Ibrahim, A. A., M. A. Abdalla, A. B. Abdel-Rahman, and H. F. Hamed, "Compact MIMO antenna with optimized mutual coupling reduction using DGS," *International Journal of Microwave and Wireless Technologies*, Vol. 6, No. 2, 173, 2014.
13. Toktas, A. and A. Akdagli, "Compact multiple-input multiple-output antenna with low correlation for ultra-wide-band applications," *IET Microwaves, Antennas & Propagation*, Vol. 9, No. 8, 822–829, 2015.
14. Liu, L., S. W. Cheung, and T. I. Yuk, "Compact multiple-input-multiple-output antenna using quasi-self-complementary antenna structures for ultrawideband applications," *IET Microwaves, Antennas & Propagation*, Vol. 8, No. 13, 1021–1029, 2014.
15. Abdelaziz, A. and E. K. Hamad, "Isolation enhancement of 5G multiple-input multiple-output microstrip patch antenna using metamaterials and the theory of characteristic modes," *International Journal of RF and Microwave Computer-Aided Engineering*, Vol. 30, No. 11, e22416, 2020.
16. Zou, X.-J., G.-M. Wang, Y.-W. Wang, and H.-P. Li, "An efficient decoupling network between feeding points for multielement linear arrays," *IEEE Transactions on Antennas and Propagation*, Vol. 67, No. 5, 3101–3108, 2019.
17. Ki Hamad, E. and M. Zm Hamdalla, "Design of miniaturized and high isolation metamaterial-based MIMO antenna for mobile terminals," *JES. Journal of Engineering Sciences*, Vol. 45, No. 6, 763–772, 2017.
18. Zhao, A. and Z. Ren, "Size reduction of self-isolated MIMO antenna system for 5G mobile phone applications," *IEEE Antennas and Wireless Propagation Letters*, Vol. 18, No. 1, 152–156, 2018.
19. Ren, Z. and A. Zhao, "Dual-band MIMO antenna with compact self-decoupled antenna pairs for 5G mobile applications," *IEEE Access*, Vol. 7, 82288–82296, 2019.

20. Yang, Z., J. Xiao, and Q. Ye, "Enhancing MIMO antenna isolation characteristic by manipulating the propagation of surface wave," *IEEE Access*, Vol. 8, 115 572–115 581, 2020.
21. Nakmouche, M. F., A. Allam, D. E. Fawzy, D. B. Lin, M. Fathy, and A. Sree, "Development of H-slotted DGS based dual band antenna using ann for 5G applications," *15th Eur. Conf. Antennas Propag. (EuCap)*, 2021.
22. Nakmouche, M. F., A. Allam, D. E. Fawzy, and D. B. Lin, "Low profile dual band H-slotted DGS based antenna design using ann for K/Ku band applications," *International Conference on Electrical & Electronics Engineering*, 2021.
23. Nakmouche, M. F. and M. Nassim, "Impact of metamaterials DGS in PIFA antennas for IOT terminals design," *2019 6th International Conference on Image and Signal Processing and Their Applications (ISPA)*, 1–4, IEEE, 2019.
24. Nakmouche, M. F., D. E. Fawzy, A. Allam, H. Taher, and M. F. A. Sree, "Dual band SIW patch antenna based on H-slotted DGS for Ku band application," *2020 7th International Conference on Electrical and Electronics Engineering (ICEEE)*, 194–197, IEEE, 2020.
25. Mahlaoui, Z., A. Latif, A. Hussaini, I. Elfergani, A. Ali, F. Mirza, and R. Abd-Alhameed, "Design of a Sierpinski patch antenna around 2.4 GHz/5 GHz for WiFi (ieee 802.11 n) applications," *2015 Internet Technologies and Applications (ITA)*, 472–474, IEEE, 2015.
26. Goyal, N., S. S. Dhillon, and A. Marwaha, "Hybrid fractal microstrip patch antenna for wireless applications," *2015 1st International Conference on Next Generation Computing Technologies (NGCT)*, 456–461, IEEE, 2015.
27. Mandelbrot, B. B., "Stochastic models for the earth's relief, the shape and the fractal dimension of the coastlines, and the number-area rule for islands," *Proceedings of the National Academy of Sciences*, Vol. 72, No. 10, 3825–3828, 1975.
28. Kaur, M. and J. S. Sivia, "Ann and FA based design of hybrid fractal antenna for ISM band applications," *Progress In Electromagnetics Research C*, Vol. 98, 127–140, 2020.
29. Cohen, N., "Fractal antenna and fractal resonator primer," *Benoit Mandelbrot: A Life in Many Dimensions*, 207–228, World Scientific, 2015.
30. Mezaal, Y. S., "New compact microstrip patch antennas: Design and simulation results," *Indian Journal of Science and Technology*, Vol. 9, No. 12, 1–6, 2016.
31. Kubacki, R., M. Czy_zewski, and D. Laskowski, "Minkowski island and crossbar fractal microstrip antennas for broadband applications," *Applied Sciences*, Vol. 8, No. 3, 334, 2018.
32. Sultan, K. S. and H. H. Abdullah, "Planar UWB MIMO-diversity antenna with dual notch characteristics," *Progress In Electromagnetics Research C*, Vol. 93, 119–129, 2019.
33. Sharawi, M. S., "Current misuses and future prospects for printed multiple-input, multiple-output antenna systems [wireless corner]," *IEEE Antennas and Propagation Magazine*, Vol. 59, No. 2, 162–170, 2017.
34. Wang, F., Z. Duan, X. Wang, Q. Zhou, and Y. Gong, "High isolation millimeter-wave wideband MIMO antenna for 5G communication," *International Journal of Antennas and Propagation*, Vol. 2019, 2019.
35. Sun, Y.-X. and K. W. Leung, "Substrate-integrated two-port dual-frequency antenna," *IEEE Transactions on Antennas and Propagation*, Vol. 64, No. 8, 3692–3697, 2016.
36. Zhang, Y., J.-Y. Deng, M.-J. Li, D. Sun, and L.-X. Guo, "A MIMO dielectric resonator antenna with improved isolation for 5G mm-wave applications," *IEEE Antennas and Wireless Propagation Letters*, Vol. 18, No. 4, 747–751, 2019.
37. Khalid, M., S. Iffat Naqvi, N. Hussain, M. Rahman, S. S. Mirjavadi, M. J. Khan, Y. Amin, et al., "4-port MIMO antenna with defected ground structure for 5G millimeter wave applications," *Electronics*, Vol. 9, No. 1, 71, 2020.
38. Iqbal, A., A. Basir, A. Smida, N. K. Mallat, I. Elfergani, J. Rodriguez, and S. Kim, "Electromagnetic bandgap backed millimeter-wave MIMO antenna for wearable applications," *IEEE Access*, Vol. 7, 111135–111144, 2019.

39. Hussain, N., M.-J. Jeong, J. Park, and N. Kim, "A broadband circularly polarized Fabry-Perot resonant antenna using a single-layered PRS for 5G MIMO applications," *IEEE Access*, Vol. 7, 42 897–42 907, 2019.
40. Jiang, H., L.-M. Si, W. Hu, and X. Lv, "A symmetrical dual-beam bowtie antenna with gain enhancement using metamaterial for 5G MIMO applications," *IEEE Photonics Journal*, Vol. 11, No. 1, 1–9, 2019.
41. Al Abbas, E., M. Ikram, A. T. Mobashsher, and A. Abbosh, "MIMO antenna system for multi-band millimeter-wave 5G and wideband 4G mobile communications," *IEEE Access*, Vol. 7, 181 916–181 923, 2019.
42. Iffat Naqvi, S., N. Hussain, A. Iqbal, M. Rahman, M. Forsat, S. S. Mirjavadi, and Y. Amin, "Integrated LTE and millimeter-wave 5G MIMO antenna system for 4G/5G wireless terminals," *Sensors*, Vol. 20, No. 14, 3926, 2020.
43. El Hadri, D., A. Zakriti, A. Zugari, M. El Ouahabi, and J. El Aoufi, "High isolation and ideal correlation using spatial diversity in a compact MIMO antenna for fifth-generation applications," *International Journal of Antennas and Propagation*, Vol. 2020, 2020.